Journal of Power Sources 196 (2011) 835–846

Contents lists available at ScienceDirect

Journal of Power Sources

journal homepage: www.elsevier.com/locate/jpowsour

Intelligent power management in a vehicular system with multiple power sources☆

Yi L. Murphey[a], ZhiHang Chen[a,*], Leonidas Kiliaris[a], M. Abul Masrur[b]

[a] Department of Electrical and Computer Engineering at the University of Michigan-Dearborn, 4901 Evergreen Rd., Dearborn, MI 48128, USA
[b] U.S. Army RDECOM-TARDE, Warren, MI, USA

ARTICLE INFO

Article history:
Received 7 May 2010
Received in revised form 19 July 2010
Accepted 20 July 2010
Available online 30 July 2010

Keywords:
Electric power management
Vehicular power system
Energy management
Power demand duty cycle

ABSTRACT

This paper presents an optimal online power management strategy applied to a vehicular power system that contains multiple power sources and deals with largely fluctuated load requests. The optimal online power management strategy is developed using machine learning and fuzzy logic. A machine learning algorithm has been developed to learn the knowledge about minimizing power loss in a Multiple Power Sources and Loads (M_PS&LD) system. The algorithm exploits the fact that different power sources used to deliver a load request have different power losses under different vehicle states. The machine learning algorithm is developed to train an intelligent power controller, an online fuzzy power controller, FPC_MPS, that has the capability of finding combinations of power sources that minimize power losses while satisfying a given set of system and component constraints during a drive cycle. The FPC_MPS was implemented in two simulated systems, a power system of four power sources, and a vehicle system of three power sources. Experimental results show that the proposed machine learning approach combined with fuzzy control is a promising technology for intelligent vehicle power management in a M_PS&LD power system.

1. Introduction

In recent years, advanced diesel engines, fuel cells, and hybrid powertrains have been actively studied as promising technologies for future ground vehicles because of their potential to significantly improve fuel economy and reduce emissions. It is likely that future ground vehicles will have a hybrid of multiple power sources [1,2]. A hybrid of multiple power sources naturally has more complex configuration and varieties of operation modes. Therefore the power control strategy of a hybrid vehicle has more impact on fuel efficiency than a conventional vehicle.

There have been increased research activities in vehicle power management [3] in recent years. Most of the vehicle power management approaches were developed based on mathematical models, human expertise, or knowledge derived from simulation data. The application of optimal control theory to power distribution and management has been the most popular approach. Linear programming [4], optimal control [5–7], and especially dynamic programming (DP), have been widely studied and applied to a broad range of vehicle models [8–11]. However, most of these techniques do not offer an on line solution, because they assume that the future information in a driving cycle is entirely known. The results generated by these techniques have been used primarily as performance benchmarks. Intelligent systems approaches such as neural networks, fuzzy logic and genetic algorithms have also been explored for intelligent power management in hybrid electrical vehicles [12–20] as well as in conventional vehicles [3,10,21].

This paper presents an intelligent power management approach for a vehicular power system that has multiple power sources. In recent years, multiple power sources have been employed in trucks and vehicles with the aim of achieving overall energy efficiency. Typical power sources used in vehicles include internal combustion engines, fuel cells, ultracapacitors, batteries, etc. [2,3,15]. The hybrid vehicles with multiple power sources have the advantage of requesting the necessary power from the best combination of power sources in terms of energy efficiency during a drive cycle. The research presented in this paper focuses on developing machine learning algorithms for learning optimal power control within a hybrid vehicle system that has three or more energy sources and large load fluctuations. Examples of such vehicles are heavy trucks, construction and utility vehicles, and military trucks and vehicles [1,22,23]. Dynamically selecting a combination of power sources can offer new opportunities to minimize the fuel consumption of the internal combustion engine used in these vehicles.

☆ This work was supported in part by the U.S. Army RDECOM-TARDEC under the contract DAAEO7-03-C-L098.
* Corresponding author. Tel.: +1 313 593 5464; fax: +1 313 583 6336.
E-mail address: zhchen@umich.edu (Z. Chen).

0378-7753/$ – see front matter © 2010 Elsevier B.V. All rights reserved.
doi:10.1016/j.jpowsour.2010.07.052

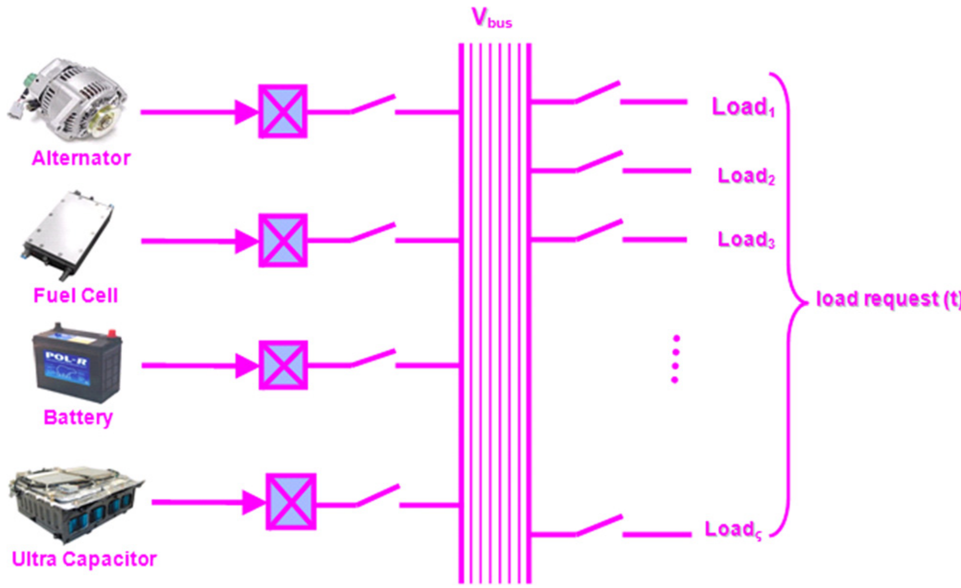

Fig. 1. A schematic diagram of a M_PS&LD system.

A generic multiple power sources and loads (M_PS&LD) system architecture is proposed to address the issues of intelligent power management. A machine learning algorithm, MLOPS (Machine Learning Optimal Power Sources), is developed to learn from training data the knowledge about the optimal power management for a broad range of possible power requests with constraints related to the system voltage and the state of charge (SOC) of power storage units, e.g. batteries and ultracapacitors. Specifically, MLOPS addresses the following issues. For a given request of electric loads,

- find the optimal power source combination to deliver the load with respect to minimizing the overall system power loss;
- keep the SOCs of energy storage units within the pre-defined threshold margins;
- minimize bus voltage fluctuation.

FPC_MPS is an online fuzzy power controller based on the knowledge about selecting optimal power sources learnt by MLOPS for a given request of electric loads. Both the MLOPS and the FPC_MPS have been fully implemented in a simulation software environment. The machine learning algorithm and the FPC_MPS have been tested on the simulation data generated by two types of vehicular power systems. One is a system with four power sources, namely, an alternator, fuel cell, an ultracapacitor and a battery, developed under a generic simulation environment [24] that can take highly fluctuated loads. The other is a HEV model using a high fidelity vehicle simulation software [25] developed by Argonne National Laboratory under the direction of and with contributions from major automotive companies. The HEV has an engine, an alternator, an ultracapacitor and a battery. The experimental results show that the well trained FPC_MPS implemented in both systems is able to reduce power loss by 28–76% in comparison with a power controller that uses all power sources at all times.

This paper is organized as follows. Section 2 presents the M_PS&LD vehicle power system architecture and the definition of the power management problem under this study. Section 3 introduces the machine learning algorithm, MLOPS (Machine Learning Optimal Power Sources). Section 4 presents the online fuzzy power controller, FPC_MPS. Section 5 presents the experiment results and Section 6 concludes the paper.

2. A vehicle system of multiple power sources and loads

Fig. 1 presents the schematic drawing of a M_PS&LD system. A system voltage bus, V_{bus}, with 42-V, is used to connect the power sources to the electric loads. The multiple power sources connecting to V_{bus}, are controlled electronically to have two states, *off* and *on*. When a power source is in the *on* state, it is connected to V_{bus}, and disconnected from V_{bus} when in the *off* state. In the case of an alternator with a diode, V_{bus} controller only allows power to flow from the alternator to the bus and not in the reverse direction. In this figure, for the sake of illustration, four power sources are shown, alternator (alt), fuel cell (fc), battery (bat) and ultracapacitor (ucap). More and/or other types of power sources can be added to the system. For the convenience of description, we will use this M_PS&LD as an example throughout the paper.

The four power sources shown in Fig. 1 are the most commonly used energy sources in vehicles. The charging of battery and ultracapacitor is from the alternator. The alternator, also called generator, is directly coupled to an internal combustion engine's crankshaft. It can be used to charge the battery and/or ultracapacitor, thus help to maintain a stable voltage level on the power net. So, controlling its output power leads to change in the operating point of the combustion engine, and thus affects the fuel consumption.

The most popular fuel cell for vehicle applications is an electrochemical device that combines hydrogen and oxygen to produce electricity, with water and heat as its by-product. As long as fuel is supplied, the fuel cell will continue to generate power. Since the conversion of the fuel to energy takes place via an electrochemical process, unlike combustion, the process is clean, quiet and highly efficient compared to fuel burning. For that reason, the making of a practical automobile that uses the fuel cell as a power source has been actively pursued in the recent years, in particular in HEV trucks [26–28]. Traditional lead–acid batteries have been present in vehicles for many years to supply key-off loads and, sometimes, continuous load requirements when the alternator itself may not be able to do so efficiently [10]. Ultracapacitors are energy storage devices that use electrolytes configured by various-sized cells into modules to meet the power, energy, and voltage requirements for a wide range of applications. Although, ultracapacitors are more expensive (per energy unit) than batteries, they have a much greater instantaneous power capability compared to batteries of similar physical size [2,15]. An ultracapacitor can

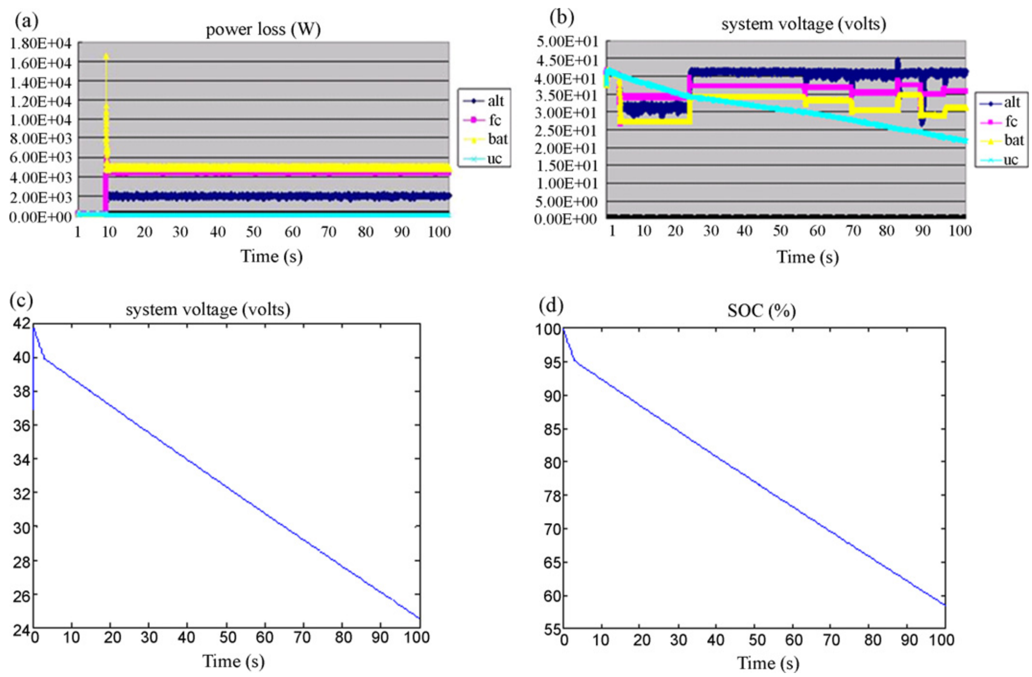

Fig. 2. Analysis of power loss, bus voltage and SOC of four individual power sources. (a and b) The instantaneous power losses and system voltage generated by four simulations, each of which uses one of the four power source. (c and d) The system bus voltage and the SOC_{ucap} when an ultracapacitor is the only power source used during the simulation.

receive regenerative energy and give power during peak periods. Moreno et al. [15] proposed to use an ultracapacitor as an auxiliary energy system in combination with a primary source that is unable to accept energy from the regenerative braking. There are other power sources being considered in HEV research [3,15,28], and future vehicle systems may use combinations of these power sources and those shown in Fig. 1.

In this M_PS&LD, multiple power loads, automotive and/or equipment, are connected to the V_{bus}. Each load has two states, *off* and *on*, representing the state of being disconnected or connected

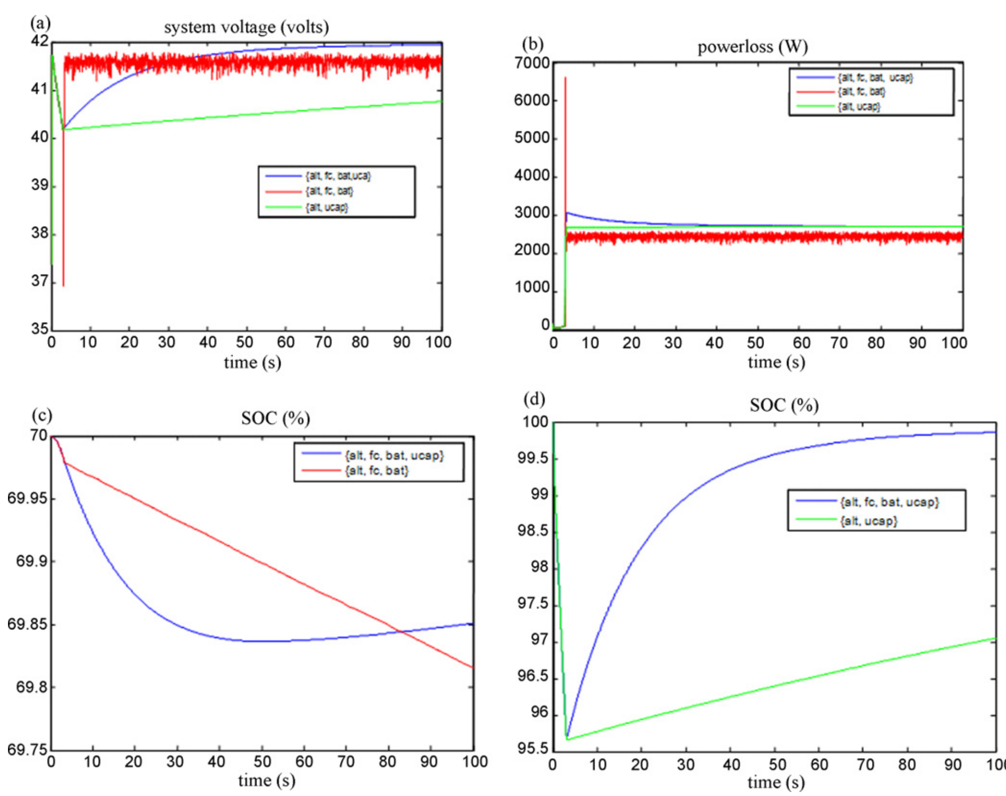

Fig. 3. Analysis of power loss, system voltage and SOC's generated by various power source combinations for the same load request of 13,724 W. (a) System voltage during the simulations, (b) the instantaneous power loss during the simulations, (c and d) the SOC of the battery and the SOC of the ultracapacitor, respectively, during the simulation.

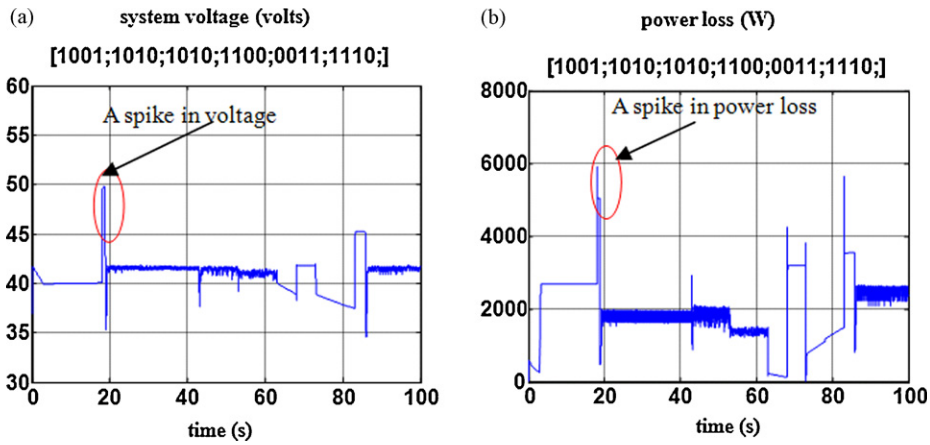

Fig. 4. Illustration of surge in voltage and power loss. (a) System voltage during the simulation. (b) Instantaneous power loss (measured in watt) during the simulation.

to V_{bus}, respectively. At any given time a load request is the collection of all loads that are in the "on" state, i.e. connected to V_{bus}. The total load request $Ld(t)$ is delivered by the m power sources currently connected to V_{bus}.

From the perspective of power management, a drive cycle (DC) is modeled as a sequence of load requests in the time domain, and the power management problem in a M_PS&LD system is defined as follows. A vehicle power system, V is a function of P_S and L_RQ, where P_S = $\{p_1, \ldots, p_\rho\}$, is a set of ρ power sources available in V, L_RQ = $\{\ell_1, \ldots, \ell_L\}$ is a set of L loads in V, which include both propulsion and non-propulsion loads. A drive cycle (DC) is defined as a sequence of load requests over a particular time period, i.e. DC $= \{Ld(t_k) | Ld(t_k) = \sum_{j=1}^{r_k} l_j^{t_k}, \{l_1^{t_k}, l_2^{t_k}, \ldots, l_{r_k}^{t_k}\} \subseteq$ L_RQ, $\quad k = 0, \ldots, N-1\}$. Each load request $Ld(t_k)$ is the summation of the loads requested by the vehicle system during time interval, $[t_k, t_{k+1})$, for $k = 0, 1, \ldots, N-1$, where $t_0 = 0$, and $t_N = t_e$ is the ending time of the drive cycle. Please note the time intervals have various lengths depending on the arrival of new load requests.

A drive cycle begins with a specific electric load for the start of the vehicle, denoted as "start", and ends with a specific electric load, denoted as "stop," which is used to turn off the vehicle. The amounts of power requested by "start" and "stop" operations are vehicle dependent but not drive cycle dependent. For the ease of description, we will ignore these two load requests during optimization to assume driver's load requests begins at time $t = 0$ and ends at $t = t_e$.

This research focuses on the development of an intelligent power management system, F, that makes an intelligent decision at every time step t during a drive cycle on the optimal power sources that should be used by V in order to minimize cost. It should be noted that the term "cost" here is used in a mathematical sense, implying that the value of a certain quantity (i.e. the "cost") will be higher if certain predetermined attributes in the system are exceeded. This can be actual fuel quantity or energy, or it can imply other things like exceeding some threshold current or state of charge (SOC), etc. F can be defined formally as follows. $F(Ld(t_k)$, V_S$(t_k), C_1, \ldots, C_\rho | \Psi) = ps^{op}(t_k) \subseteq$ P_S such that V generates minimal cost when $ps^{op}(t_k)$ is used at time step t_k for the given load request $LR(t_k)$ under the current vehicle power system state V_S(t_k). V_S(t_k) is a vector of SOCs of the power storages used as power sources in the system, C_i is the cost function associated with ith power source p_i in P_S, Ψ is a set of operation constraints of the power system such as the stability of the voltage at V_{bus} and the optimal operation ranges of the individual components in the power system.

The development of F is formulated as the optimization problem of finding $ps^{op}(t_k)$ at each time step t_k through a drive cycle DC. The objective function is defined as follows:

$$\underset{\overline{PS}}{\text{Min}}\ J = \sum_{k=0}^{N} \underset{ps^{op}(t_k)}{\text{Min}} \{\gamma(ps(t_k)|Ld(t_k), \text{V\_S}(t_k))\},$$
$$\times \text{ subject to constraints in } \Psi, \qquad (1)$$

where $t_N = t_e$, $\gamma(ps(t_k)|Ld(t_k)$, V_S$(t_k))$ is the power loss when power sources in $ps(t_k)$ are used at time t_k in the vehicle power state

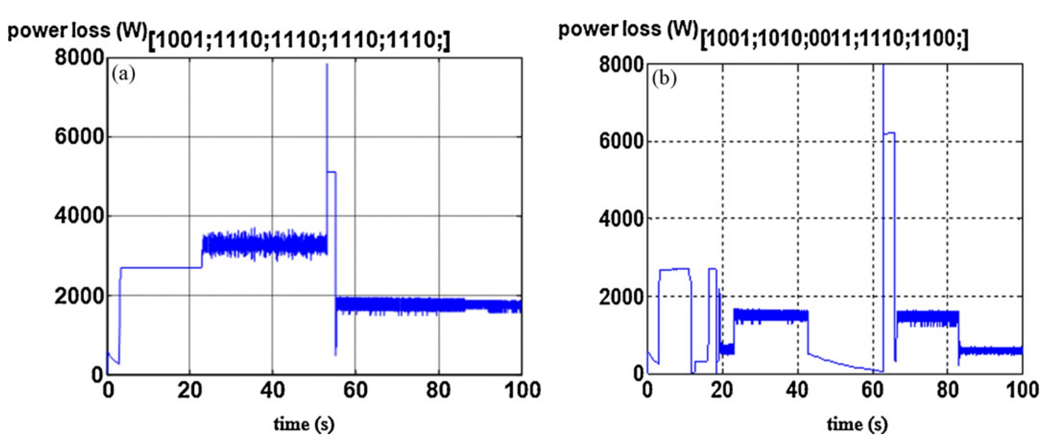

Fig. 5. Power loss surges in two drive cycles specified in Table 2: (a) load requests change but no changes in power sources and (b) no load request changes but changes in power sources.

Table 1
Drive cycle used in generating results shown in Fig. 4.

Time (s)	0–3	3–18	18–43	43–53	53–63	63–68	68–73	73–78	78–83	83–100
Load request	Start mode	13,724 W	3755 W	6073 W	9233 W	6080 W	5653 W	11,523 W	10,573 W	5930 W
Power source combination (binary combination for power source)	0011	1001	1010	1010	1100	0011	1110	0101	0111	1010

V_S(t_k) to deliver power to the load request $Ld(t_k)$, and $\overline{PS} = (ps^{op}(t_0), \ldots, ps^{op}(t_N))$.

Since the power loss function under consideration is a nonlinear system, it is difficult to optimize the system using closed form equations. Thus the optimization problem is solved through a machine learning process described in Section 3.

3. Machine learning about load-based optimal power delivery

This section presents the description of the load-based optimal power delivery, the heuristic knowledge about systems of multi-power sources, and the machine learning algorithm, MLOPS.

3.1. Optimal power delivery in a drive cycle

For ρ power sources there are M possible power source combinations that can be used to deliver power to a load request $Ld(t_k)$,

$$M = \sum_{i=1}^{\rho} \binom{\rho}{i} = \sum_{i=1}^{\rho} \frac{\rho!}{i!(\rho - i)!} \quad (2)$$

The power optimization scheme presented in this paper builds upon the fact that different power source combinations bear different power losses and generate different impacts to the power system. This paper presents a machine learning approach to solve the problem. A machine learning algorithm, MLOPS is developed to train an intelligent power management function F that satisfies the following constraints.

1. The state of charge (SOC) of every energy storage should stay within the specified bounds, i.e. L_B(ε_i) ≤ SOC(ε_i) ≤ U_B(ε_i), i = 1, . . ., g, where ε_i is a power source in P_S and also a power storage unit such as battery or ultracapacitor, and L_B(ε_i) and U_B(ε_i) are the lower and upper bounds of ε_i, respectively.
2. The system voltage should be kept within a bound, i.e. LB_V ≤ $V_{bus}(t_k)$ ≤ UB_V, so it is not too high to cause damage nor too low to supply sufficient power, where LB_V and UB_V are the lower and upper bound for the system voltage.
3. When load request and/or power source combination changes, the system voltage should be kept stable. It can be specified quantitatively as

$$|V_{bus}(t_k) - V_{bus}(t_{k-1})| \leq \tau, \quad \text{where } \tau > 0 \text{ is a threshold.} \quad (3)$$

The power loss function is defined as

$$\gamma(ps(t_k)|Ld(t_k), V\_S(t_k)) = \sum_j P^j_{loss}(Ld(t_k), \mathrm{V\_S}(t_k)), \quad (4)$$

where P^j_{loss}, the power loss function of the jth power source in $ps(t_k)$. For a given load request $Ld(t_k)$ and a vehicle power state V_S(t_k), the power loss function is calculated as follows:

$$P^j_{loss}(Ld(t_k), \mathrm{V\_S}(t_k)) = P^j_g - P^j_r, \quad \text{and} \quad \sum_j^{\rho} P^j_r = Ld(t_k), \quad (5)$$

where P^j_g and P^j_r are the generated and requested power from the jth power source, respectively. When $P^j_r = 0$, there is no power drawn from the jth power source, which implies $P^j_g = 0$ and $P^j_{loss} = 0$. It is reasonable to assume that a simulated or a physical vehicle system provides P^j_g when a power request P^j_r is made. Note that the power loss function may be extended to include several costs such as cost of charging, wearing and emission. But in this paper we focus on minimizing power loss. The vehicle power state, V_S(t_k) is defined by the SOCs of the power sources and the voltage at the power bus. For the system shown in Fig. 1, V_S(t_k) = {SOC$_{ucap}(t_k)$, SOC$_{bat}(t_k)$, $V_{bus}(t_k)$}.

The MLOPS algorithm is developed based on the behavior of the M_PS&LD vehicle systems analyzed as follows. Figs. 2–5, generated by the power system shown in Fig. 1 implemented in a simulation environment, illustrate various characteristics of the M_PS&LD vehicle system.

- For the same given load request different power sources have different power losses. Fig. 2 shows the results of four simulations, each using a single power source to provide the same power request of 13,724 W. This particular numerical value is merely due to the particular combination of loads used and is not of significance in itself. Fig. 2(a) shows the accumulative power loss curves generated by the four simulations. The dark blue curve represents the power loss when the alternator was used, the pink curve is when the fuel cell was used, the yellow curve is when the battery was used, and the light blue curve is when the ultracapacitor was used. (For interpretation of the references to color in this sentence, the reader is referred to the web version of the article.)
- The vehicle state should be strictly monitored and be part of the constraints during the minimization of power loss. For example, Fig. 2(a) shows that the ultracapacitor had the least power loss while providing the same amount of power. However, Fig. 2(b) shows that when the ultracapacitor was used alone, the system voltage, V_{bus} was plummeting during the simulation and ended at 25 W. When the simulation continued for 350 min, the voltage of the system bus and the SOC of the ultracapacitor all dropped

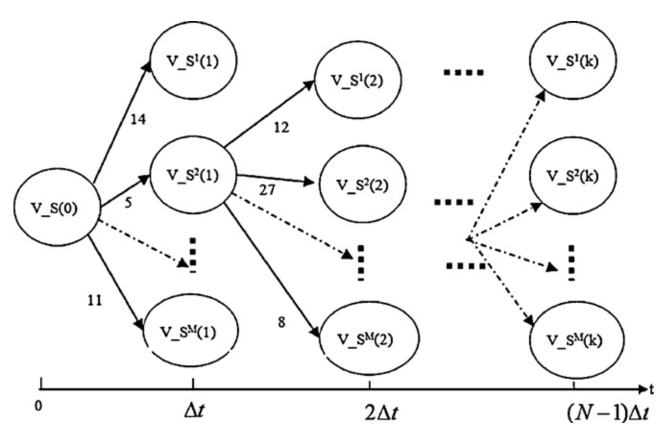

Fig. 6. Finding optimal power source combinations by looking for the least cost path throughout a drive cycle.

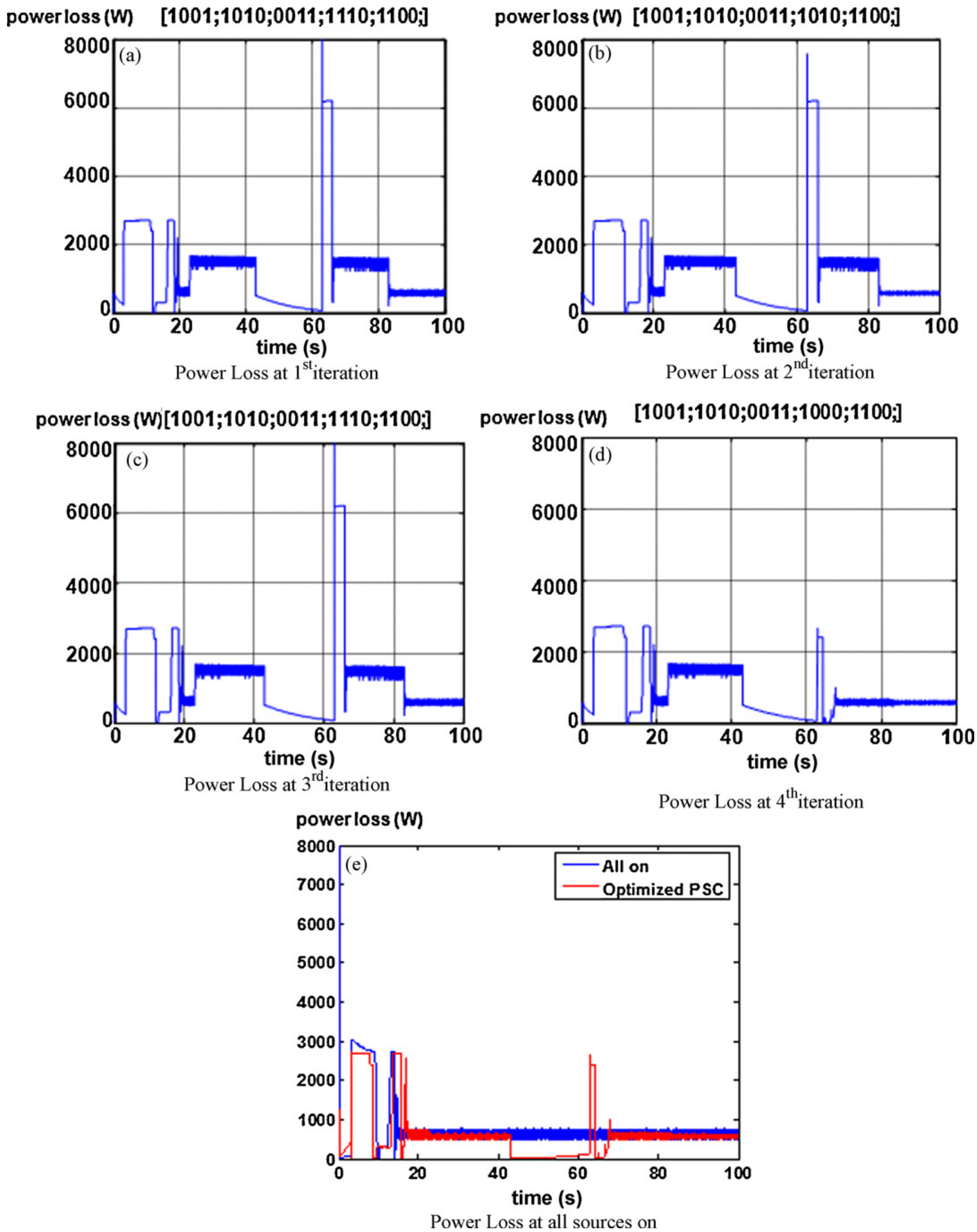

Fig. 7. Illustration of computations in MLOPS. (a) Power loss during 1st iteration, (b) power loss during 2nd iteration (c) power loss during 3rd iteration, (d) power loss during 4th iteration (e) Power loss with all sources on throughout the drive cycle.

to 0 (see Fig. 2(c and d)). In order to avoid getting into this type of situations, the optimization process must include constraints represented by the variables in power system state as discussed above.

- Different power source combinations likely give different power losses for the same load request. Fig. 3 illustrates a few examples. For the same load request, three different power source combinations were used in three simulation runs: (1) all power sources were turned on, denoted as {alt, fc, bat, ucap}, (2) a three power source combination, denoted as {alt, fc, bat}, was used, and (3) a two power source combination, denoted as {alt, ucap}, was used. In this example, the three power source combination gave the best performance: lowest power loss while the bus voltage and the SOC of the battery were kept within bounds (see Fig. 3(c)). The two power source combination gave the least power loss while keeping the bus voltage and the SOC of the ultracapacitor high (see Fig. 3(d)).
- Power loss is not only a function of power requested, but also of the SOC's of the power storage units such as batteries and ultracapacitors and many other factors including temperature and aging. Therefore, it is not easy to model power loss functions in explicit mathematic forms.
- When load request changes and/or power source combination changes, there could be a sudden rise and drop at the voltage bus. This causes a power loss surge in the system. We define such events as spikes. A spike in a function, whether a voltage function or a power loss function, is where the function has a steep rise followed immediately by a big fall. Fig. 4 shows the voltage and power loss generated by a drive cycle specified in Table 1. For the convenience of description, the power source combinations are

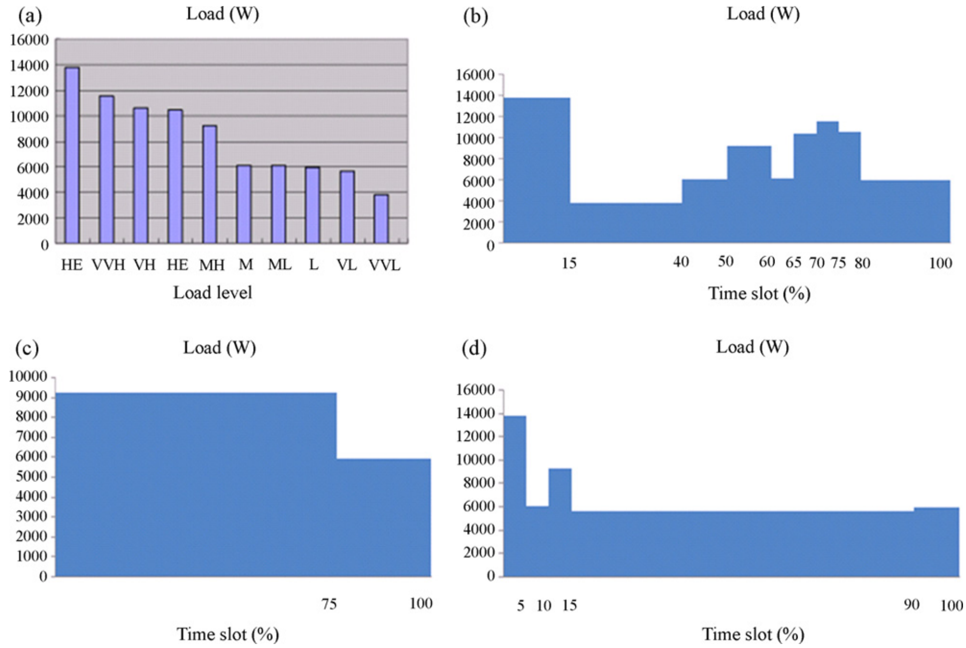

Fig. 8. Load requests and drive cycles used in experiments. (a) The 10 levels of load requests, (b) drive cycle DC1, (c) drive cycle DC2 and (d) drive cycle DC3.

coded in a 4-bit binary string $b_1b_2b_3b_4$, where b_1 represents state of alternator, b_2 fuel cell, b_3 the battery, b_4 the ultracapacitor. $b_i = 0$, $i = 1$–4, indicates its corresponding power source is "off", otherwise it is "on". From Fig. 4(a), we observe a spike in voltage, and in Fig. 4(b) a spike in power loss. Both spikes occurred at the same time, $t = 18$ s. At that time the load request changed from 13,724 W to 3755 W, and the power source combination also changed from {alt, uc} to {alt, bat}. We observed repeatedly in many experiments that every time there is a spike in system voltage, there is also a corresponding spike in power loss. These spikes cause instability in system voltage, and large amount of power loss. Therefore a power management system should avoid these spikes. Since our focus is to minimize power loss, we attempt to minimize all spikes in power loss functions, including the power loss spike occurred at $t = 83$ (see Fig. 4(b)). Fig. 5 shows power loss spikes occurring in two different scenarios: (a) a spike occurred at $t = 53$ s, when the load request changed from 13,724 W to 3755 W, but the power source combination stayed the same; (b) a power loss spike occurred at $t = 63$ s, when the power source combination changed from {bat, uc} to {alt, fc, bat} but the load request remained the same.

Based on the analysis above, we developed the machine learning algorithm described in the next section.

3.2. Machine learning about optimal power source combinations

The machine learning algorithm, MLOPS, is developed to learn knowledge that can be used by an online power controller to make intelligent decisions about selecting a power source combination during a drive cycle while satisfying the practical constraints of vehicle components and maintaining uninterrupted power availability and system stability. The algorithm is designed as follows:

- Defining a set of frequently occurred load requests, L_RQ = $\{\ell_1, \ldots, \ell_L\}$, where ℓ_i is a combination of the loads shown in Fig. 1, which should include propulsion and non-propulsion loads.
- Construct a drive cycle using an every single load request ℓ_i, i.e. $DC_i = \{ld(k\Delta t) = \ell_i | k = 0, \ldots, N-1\}$, $i = 1, \ldots, L$.
- Implementing the M_PS&LD system in a high fidelity simulation program ξ such that ξ has
  - accurate functions to calculate power consumption and power loss for each power source for a given load request and dynamically update vehicle power state during a drive cycle;
  - a control mechanism to allow any power sources to be connected or disconnected from the voltage bus. The set of power source combinations is denoted as PSC = $\{pc_1, pc_2, \ldots, pc_M\}$, where $M = 2^{\rho}$;
  - real time functions, $V_{bus}(t)$ for calculating system voltage, $SOC_1(t), \ldots, SOC_g(t)$ for calculating state of charge for the g power storage units used in the system.

MLOPS builds a knowledge base that contains optimal power source combinations for various load requests under various vehicle power states. The knowledge base will be used to train the fuzzy online controller described in the next section. The major computational steps of MLOPS are presented as follows.

3.2.1. Algorithm of machine learning about optimal power sources (MLOPS)

Input variables: power source combinations, $PSC = \{pc_1, pc_2, \ldots, pc_M\}$; load requests, L_RQ = $\{\ell_1, \ldots, \ell_L\}$;

Initial values of the SOCs and the system voltage: $Init\_SOC_{\varepsilon_1}, \ldots, Init\_SOC_{\varepsilon_g}, Init\_V_{bus}$;

Output variables: matrices contain optimal power source combinations and the corresponding system voltage and the SOCs of all power storages, OP_PSC; OP_V_{bus}, $OP\_SOC_{\varepsilon_1}, \ldots, OP\_SOC_{\varepsilon_g}$.

Step 1: $i = 0$,
Step 2: If $i \le L$ go to Step 3 else output OP_PSC, OP_V_{bus}, $OP\_SOC_{\varepsilon_1}, \ldots, OP\_SOC_{\varepsilon_g}$.
Step 3: Finding the least cost power source combinations for the drive cycle, $DC_i = \{ld(k\Delta t) = \ell_i | k = 0, \ldots, N-1\}$ using the simulation

Table 2
Drive cycles used to generate results in Fig. 5.

Time (s)		0–3	3–23	23–43	43–53	53–63	63–83	83–100
Drive cycle used in (a)	Load request	Start mode	13,724 W	13,724 W	13,724 W	3755 W	3755 W	3755 W
	Power source combination	0011	1001	1110	1110	1110	1110	1110
Drive cycle used in (b)	Load request	Start mode	3755 W	3755 W	3755 W	3755 W	3755 W	3755 W
	Power source combination	0011	1001	1010	0011	0011	1110	1100

program ξ with load request ℓ_i and the initial vehicle state:

$$\mathrm{V\_S}^{op}(0) = \langle Init\_\mathrm{SOC}_{\varepsilon_1}, \ldots, Init\_\mathrm{SOC}_{\varepsilon_g}, Init\_V_{bus}\rangle.$$

Step 3.1: Set $k = 0$, PSC_candidates = PSC,
Step 3.2: Set $t = k\Delta t$ and run the simulation program ξ with the current vehicle power state V_S(t) to find the pc' in PSC_candidates that have the least power loss during the time period of $[t, t + \Delta t]$ within the drive cycle DC_i. The optimal PSC is denoted as $ps^{op}(t)$.
Step 3.3: Set the current vehicle power state V_S(t), to $\mathrm{V\_S}^{op}(k)$, the optimal vehicle state that is returned by ξ when the optimal power source combination, $ps^{op}(t)$ was used in simulation.
Step 3.4: Check system constraints. If any components in the vehicle power state V_S(t) are out of the bounds, or if there is a spike in system voltage or power loss during time interval $(t, t + \Delta t]$, remove the power source combination $ps^{op}(t)$ from PSC_candidates and then look for another power source combination by going back to Step 3.2.
Step 3.5: Store the best power source combination $ps^{op}(t)$ in OP_PSC[i, k], the respective V_S(t) to $\mathrm{OP\_V}_{bus}[i, k]$, $\mathrm{OP\_SOC}_{\varepsilon_1}[i, k], \ldots, \mathrm{OP\_SOC}_{\varepsilon_g}[i, k]$.
Step 3.6: If $k < K$, then $k = k + 1$ and go to Step 3.2. This moves the computation to the next time step in the drive cycle.

Step 4: Run another drive cycle by setting $i = i + 1$ and go to Step 2.

Step 3 in the MLOPS algorithm is the key component of the algorithm. For every load request ℓ_i, Step 3 searches for the PSC that have the minimum power loss while satisfying all the system constraints using a step by step approach along time of simulation. The search is a process of finding the shortest path as illustrated in Fig. 6. The nodes represent vehicle power states, and the arcs represent vehicle power state transitions. Each vehicle power state transition is caused by the use of a specific power source combination upon a power request. Each arc is associated with a weight, representing the cost when the vehicle changes from one vehicle power state to another. At the beginning of the drive cycle, there is only one node, which represents the initial vehicle power state.

At time $t = k\Delta t$, $k = 1, \ldots, N - 1$, there is a layer of M nodes, representing the vehicle power states generated by deploying M different PSCs at the vehicle power state, $\mathrm{V\_S}^{op}((k - 1)\Delta t)$, which is generated by the optimal PSC selected by process in Step 3 at $t = (k - 1)\Delta t$. The cost associated with the arc from node $\mathrm{V\_S}^{op}((k - 1)\Delta t)$ to $\mathrm{V\_S}^j(k\Delta t)$ is a function of power loss when power source combination pc_j used during the time interval $[(k - 1)\Delta t, k\Delta t)]$. $\mathrm{V\_S}^j(k\Delta t)$ is further being checked by Step 3.4 to make sure all the constraints are satisfied. The step size, Δt, should be carefully chosen. If it is too large, the vehicle power state may change significantly during the time interval, and power source combinations may need to be changed in order for the system to operate in an optimal mode. If Δt is too small, the simulation program ξ may take a long time to complete.

One of the computations at Step 3.4 is to check whether the vehicle system has a spike in system voltage or power loss when the power source combination $ps^{op}(t)$ is used. A spike in a system voltage function is quantified as follows. A spike exists at time t if and only if the following two conditions are satisfied: $\mathrm{Max}\{V_{bus}(t) - V_{bus}(t - t') | t' \le \mu\} > V\_T_{spike}$, and $\mathrm{Max}\{V_{bus}(t) - V_{bus}(t - t') | t' \le \mu\} > V\_T_{spike}$, where V_T_{spike} is a pre-set threshold by the system designer, $\mu > 0$ and is a small number set by the system designer. A spike in a power loss function can be similarly defined.

Fig. 7 shows an example of intermediate results generated by computational Steps 3.2 through 3.4 in several iterations. In this experiment, $\mathrm{DC}_i = \{Ld(k * 20) = 3755\,\mathrm{W} | k = 0, \ldots, 5\}$, which is a drive cycle of a constant load request. From $t = 0$ to $t = 3$, the vehicle system is in the startup mode. Each graph in Fig. 7 shows the instantaneous power loss through the drive cycle simulated by using the power source combinations selected by Steps 3.2 through 3.4 in one iteration at $t = 3$, 23, 43, 63, 83. During the first iteration (see Fig. 7(a)), at $t = 63$, the vehicle simulation program ξ changed the power source combination from (bat, uc) to (alt, fc, bat), which resulted in a spike of power loss. During the second iteration, the power source combination at $t = 63$ was changed from (bat, uc) to (alt, bat), which still resulted in a spike in power loss (see Fig. 7(b)). During the third iteration, the power source combination at $t = 63$ was changed from (bat, uc) to (alt, fc, bat), and a spike in the power loss was still there (see Fig. 7(c)). During the 4th iteration, the power source combination at $t = 63$ was changed to from (bat, uc) to (alt), then the spike in power loss was gone (see Fig. 7(d)). The output from the MLOPS was the optimal power source combination sequence OP_PSC = {(alt, uc), (alt, bat), (alt), (alt, fc)} along with the vehicle states, $\{\mathrm{V\_S}^{op}(0), \mathrm{V\_S}^{op}(3), \mathrm{V\_S}^{op}(23), \mathrm{V\_S}^{op}(43), \mathrm{V\_S}^{op}(63), \mathrm{V\_S}^{op}(83)\}$. Fig. 7(e) displays the instantaneous power loss generated using a combination of all power sources during the drive cycle and the power loss curve generated using the power source combinations produced by the MLOPS. It can be observed the system used the power source combinations generated by MLOPS had much less power loss in comparison with the system that used all four power sources throughout the drive cycle. The total power loss over the entire drive cycle in the system that used the power source combinations generated by the MLOPS algorithm was 61.999 kW, was 74.68 kW by the system that used all four power sources throughout the entire drive cycle.

By applying the machine learning algorithm MLOPS to all load requests occurring in a M_PS&LD system, we obtain a knowledge base of optimal power source combinations and the respective vehicle states, which is represented by OP_PSC, $\mathrm{OP\_V}_{bus}$, $\mathrm{OP\_SOC}_{\varepsilon_1}, \ldots, \mathrm{OP\_SOC}_{\varepsilon_g}$.

4. A fuzzy power controller

The theory of fuzzy logic is aimed at the development of a set of concepts and techniques for dealing with sources which have uncertainty, imprecision, or is incomplete. Fuzzy systems have been successful in many applications including control theory and engineering applications where gradual adjustments are necessary

Table 3
System constraints used in experiments.

	Lower bound	Upper bound
Battery	$\mathrm{LOWER_{bat}} = 40\%$	$\mathrm{UPPER_{bat}} = 90\%$,
Ultracapacitor	$\mathrm{LOWER_{ucap}} = 40\%$	$\mathrm{UPPER_{ucap}} = 95\%$
System voltage	$\mathrm{LOWER}_{\mathrm{v}\_bus} = 38\,\mathrm{W}$	$\mathrm{UPPER}_{\mathrm{v}\_bus} = 45\,\mathrm{W}$

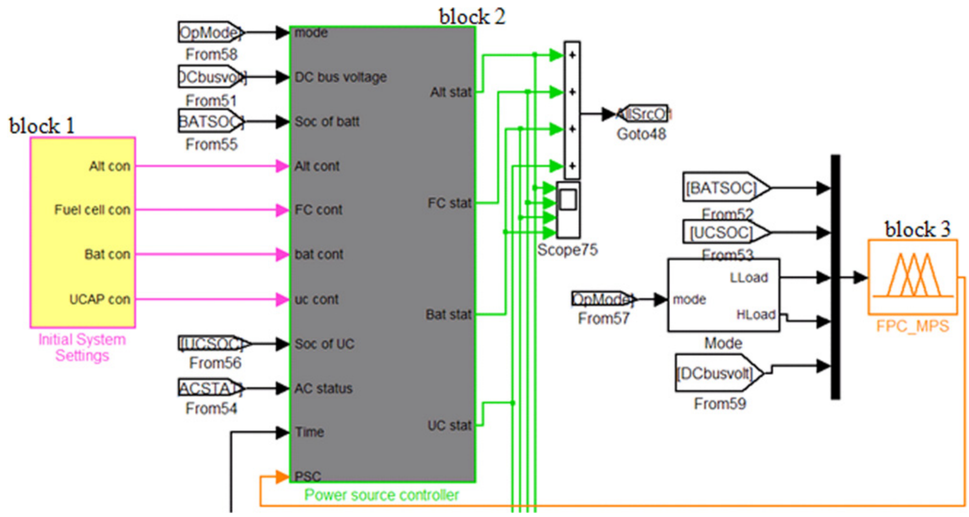

Fig. 9. Major components in a simulation model of four power sources.

[29–32]. The nature of fuzzy rules and the relationship between fuzzy sets of differing shapes provides a powerful capability for modeling a system whose complexity makes traditional expert system, mathematical, and statistical approaches very difficult. In addition fuzzy systems are easy to be understood by engineers.

For online power control, vehicle power states and power requests change gradually; therefore fuzzy logic is a promising approach. An online fuzzy power controller, FPC_MPS, has been developed and trained to select the most promising power source combinations during an online drive cycle. FPC_MPS was designed to meet the following requirements:

- For a drive cycle, power sources should be dynamically allocated and frequently so that maximum energy efficiency or minimum power loss can be achieved.
- At any time during the drive cycle, the fuzzy power controller must make sure to provide the vehicle with high performance, which is measured as follows: delivering adequate power as soon as a load request is made, and keeping the system state at the normal operation range, which means all three constraints discussed in Section 3 should be satisfied at all time.
- At any time during the drive cycle, vehicle power system should be kept stable (in terms of voltage fluctuations), i.e. voltage surges should be avoided.

To meet the above requirements, FPC_MPS generates the optimal power source combination at real time t to provide sufficient power to the load request $Ld(t)$ while the system power state V_S(t) is kept stable. FPC_MPS has one fuzzy variable to represent the system voltage, g fuzzy variables to represent state of charges of the g power storages, $SOC_{\varepsilon_1}, \ldots, SOC_{\varepsilon_g}$, used in the M_PS&LD vehicle system, and n fuzzy variables, x_i, $i = 1, \ldots, n$ to represent all possible load requests. The solution variable, y, points to PSC that is most suitable for the load request based on the current vehicle state. For the vehicle power system shown in Fig. 1, the fuzzy power controller FPC_MPS has two fuzzy variables, SOC_U and

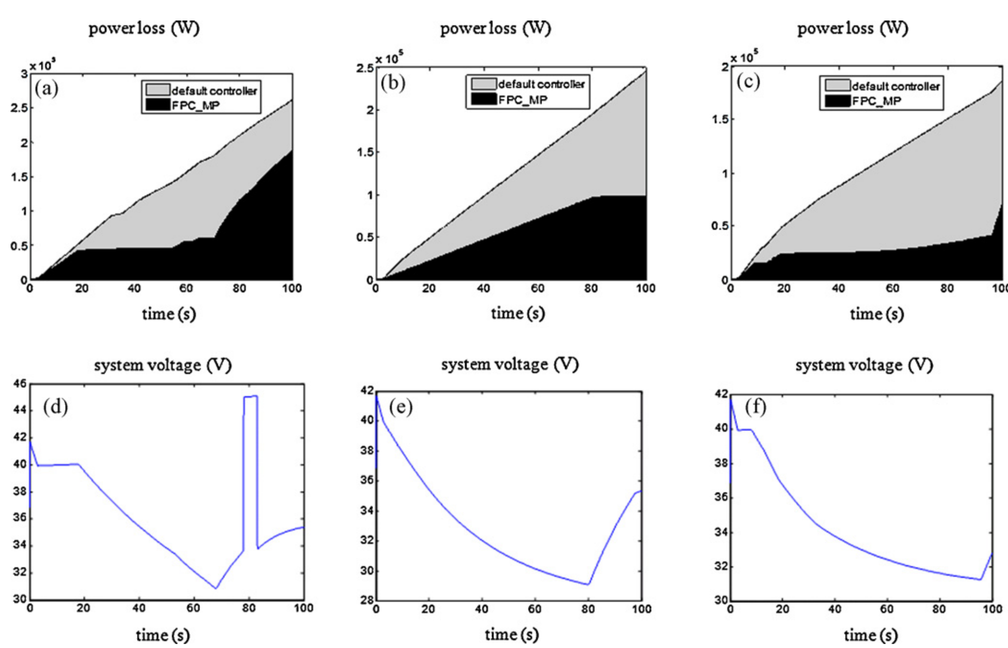

Fig. 10. Performances of FPC_MPS on three drive cycles. (a–c) The accumulative power loss during drive cycles DC1, DC2 and DC3, respectively, (d–f) the system voltage through the three drive cycles DC1, DC2 and DC3, respectively.

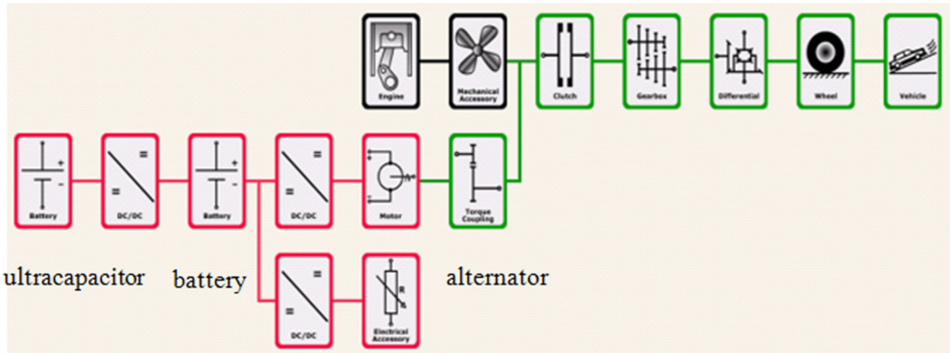

Fig. 11. A simulated vehicle model with three power sources.

SOC_B, to represent the SOC of the ultracapacitor and the batter, respectively. n, the number of fuzzy variables to represent the load requests can be determined based on the number of different load request levels the vehicle system needs to support. For a set of load requests, $L\_RQ=\{\ell_1, \ldots, \ell_L\}$, assuming, without losing generality, that $\ell_1 < \ell_2 < \ldots < \ell_L$, if each fuzzy variable x_i has η fuzzy terms, then the number of the fuzzy variables is $n = [L/\eta]$, where fuzzy variable x_1 has η fuzzy membership functions to represent load requests $\ell_1, \ldots, \ell_\eta$, x_2 has η fuzzy membership functions to represent load requests $\ell_{\eta+1}, \ldots, \ell_{2\eta}$, etc.

The fuzzy membership functions and fuzzy rules can be generated from the optimal power source knowledge generated by MLOPS algorithm using a fuzzy learning program such as the fuzzy logic toolbox provided in Matlab.

During a drive cycle, the fuzzy power controller FPC_MPS is called at a sequence of time steps. At each time step, it has the following operational steps.

- Step 1. Let the current time during a drive cycle DC be t, and assume $Ld(t)$ is the load request made by the driver.
- Step 2. Calculate the current vehicle power state $(SOC_{\varepsilon_1}(t), \ldots, SOC_{\varepsilon_g}(t))$, and fuzzify the SOC's by mapping them to the respective fuzzy membership functions.
- Step 3. Fuzzify current load request $Ld(t)$ by mapping it to the fuzzy membership functions of x_i, $i = 1, \ldots, n$.
- Step 4. Fire the fuzzy rule that are being triggered by the fuzzified $(SOC_{\varepsilon_1}(t), \ldots, SOC_{\varepsilon_g}(t))$, and $Ld(t)$. Take the consequence of the fired rule, y^* points to the optimal power source combination, ps^{op}.

5. Simulation experiments

Two sets of simulation experiments were conducted in two different simulation environments to evaluate the proposed machine learning approach for intelligent power management in a system of M_PS&LD. The first experiment was conducted by implementing the M_PS&LD power system shown in Fig. 1 in a simulation program [31]. In the second experiment, we built a vehicle model that contained three power sources using a high fidelity vehicle simulation program [32] developed by Argonne National Laboratory under the direction of and with contributions from major automotive companies. This software can simulate a broad range of pre-defined vehicle configurations (conventional, electric, fuel cell, series hybrid, parallel hybrid, and power split hybrid) (see Table 2).

The load requests used in both experiments are shown in Fig. 8(a). The machine learning algorithm, MLOPS, implemented

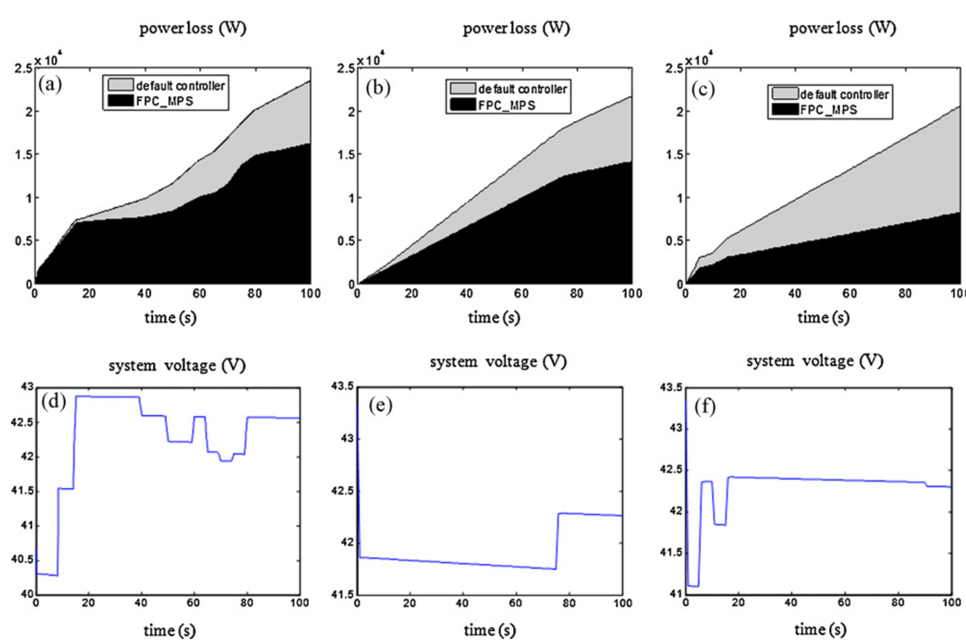

Fig. 12. Performances of FPC_MPS in a vehicle model with 3 power sources. (a–c) The accumulative power loss during drive cycles DC1, DC2 and DC3, respectively, (d–f) the system voltage through the three drive cycles DC1, DC2 and DC3, respectively 13611851008.

in VC++, generated the knowledge about the optimal power source combinations for every load request shown in Fig. 8(a) at every 10 s while satisfying all the system constraints specified in Table 3 at all time.

The fuzzy controller FPC_MPS was implemented in the simulation software [31]. FPC_MPS has two fuzzy variables, $SOC_{battery}$ and SOC_{UC}, to represent the state of charge of a battery and an ultracapacitor, respectively, one fuzzy variable, voltage, to represent the system voltage, and two fuzzy variables, x_{LLoads} and x_{HLoads} to represent the 10 load requests, where x_{LLoads} represents the five low load requests, and x_{HLoads} the 5 high load requests.

Three drive cycles were constructed to evaluate the fuzzy power controllers in both experiments (see Fig. 8(b–d)). Fig. 8(b) is a drive cycle consisting of heavy and frequently changed load requests, Fig. 8(c) is a drive cycle with low load requests and infrequent load changes, and Fig. 8(d) has more frequent load requests than the one in (b) but less than the drive cycle in (a). The following sections describe the implementations and experimental results.

5.1. A system of M_PS&LD implemented using Matlab Simulink

Fig. 9 shows the major parts of the simulation model of the M_PS&LD power system illustrated in Fig. 1 implemented in the simulation environment provided by [31]. Block 1 contains the initialization functions of the four power sources. Block 2 contains the control functions to manage the power sources. The output from FPC_MPS about the optimal power sources to use during a drive cycle is sent to block 2. Block 3 is the fuzzy power controller FPC_MPS. It receives as input the vehicle power state (i.e. SOC of battery and SOC of ultracapacitor, system bus voltage), and the current load request. If the current load request is less than the highest load level of x_{LLoads}, then it is fuzzified using the fuzzy membership functions associated with fuzzy variable *LLoad*, else it is fuzzified by fuzzy membership functions associated with fuzzy variable *HLoad*.

For every load request level shown in Fig. 10(a), a simulation was run for 100 time units and MLOPS program was called to generate the optimal power source combination from the 15 possible power source combinations at every 10 time units. The simulated power system called by MLOPS to evaluate the selected power source combinations consists of blocks 1 and 2 shown in Fig. 9. The knowledge generated by MLOPS was then used to train the fuzzy controller FPC_MPS. The performance of FPC_MPS is shown in Fig. 10(a)–(c) along with the performance of a default power controller, which uses all four power sources during the entire drive cycle. The performances are measured in terms of accumulative power loss. In all three drive cycles, the FPC_MPS had much less power loss than the default power controller. The fuzzy power controller, FPC_MPS, made 28% reduction in power loss in DC1 when compared with the power loss generated by the default controller, 60% reduction in drive cycle DC2 and 76% in DC3. The system voltage curves throughout the three drive cycles (see Fig. 10(d–f)) showed no spikes. Please note the high rise bar in the system voltage during DC1 is not a spike, since it had a stable time period.

5.2. Experiments using a simulated vehicle model

To further evaluate the proposed machine learning technologies in vehicle power systems, we constructed a vehicle model using the high fidelity simulation software [32]. Fig. 11 presents the high level view of power components in the vehicle model. The vehicle model has a conventional powertrain and three power sources, an engine and an alternator, an ultracapacitor and a battery. The engine is 4 L with the maximum power of 160 kW, and the alternator has the maximum of 14 kW in continuous mode and a peak power of 20 kW. The battery is a 42 V valve-regulated lead–acid battery with a capacity of 104 AH. The ultracapacitor is a Maxwell PC 2500 with approximately 7 kJ.

MLOPS used the simulated vehicle model in Fig. 11 to evaluate various PSCs in its learning process. For every load request shown in Fig. 10, a drive cycle was simulated with the load request as the constant electric load throughout the drive cycle and the vehicle was running at a constant speed of 40 mph. The simulation duration for each drive cycle was 100 time units, and MLOPS selected optimal PSC from evaluate power source combinations at every 10 time units. The knowledge generated by MLOPS was then used to train the fuzzy controller FPC_MPS. The FPC_MPS was evaluated on the three drive cycles shown in Fig. 10 and its performances are shown in Fig. 12. Same as in the first set of experiments, the performances are measured in terms of accumulative power loss. In all three drive cycles, the FPC_MPS had much less power loss than the default power controller. FPC_MPS resulted in 33% reduction in power loss in DC1 when compared with the power loss generated by the default controller, 63% reduction in drive cycle DC2 and 46% in DC3.

6. Conclusion

This paper presents a machine learning approach to minimizing power loss in a vehicle system of multiple power sources. A machine learning algorithm MLOPS was developed to learn about selecting optimal power source combinations for a given load request at various vehicle power states while satisfying the system constraints such as keeping the SOCs of power storages and the system voltage within specified ranges to keep it stable in the sense of low fluctuations. A fuzzy power controller, FPC_MPS, was developed for online power control. FPC_MPS was trained based on the knowledge generated by MLOPS to select a power source combination based on the given load request and vehicle power state at any given time during driving in a vehicle system of M_PS&LD. Two sets of experiments were conducted. In the first experiment, a M_PS&LD power system of four power sources was implemented using a well known simulation software [31]. In the second experiment, a M_PS&LD system of three power sources was implemented in a vehicle system using a high fidelity vehicle modeling software [32]. Both sets of experiments show that a M_PS&LD employing the FPC_MPS trained by the knowledge generated by MLOPS, can reduce power loss ranging from 28% to 76% when compared with the power controller that uses all power sources at all time without using any intelligent monitoring and control.

References

[1] M.C. Algrain, IEEE Ind. Appl. Magaz. 11 (4 (July–August)) (2005) 29–38.
[2] J.M. Miller, M. Everett, Power Electron. Trans. (2004) 19–26.
[3] Y. Murphey, Intelligent Vehicle Power Management: an Overview Studies in Computational Intelligence (SCI) 132, 169–190, www.springerlink.com.c Springer-Verlag, Berlin, Heidelberg, 2008.
[4] E.D. Tate, S. P. Boyd, Finding ultimate limits of performance for hybrid electric vehicles, SAE Paper-01-3099, 2000.
[5] M. Back, M. Simons, F. Kirschaum, V. Krebs, Proc. IFAC 15th Triennial World Congress, Barcelona, Spain, 2002.
[6] J. Bumby, I. Forster, Inst. Elect. Eng. Proc. D 134 (6 (November)) (1987) 373–387.
[7] S. Delprat, J. Lauber, T.M. Guerra, J. Rimaux, IEEE Trans. Veh. Technol. 53 (3 (May)) (2004) 872–881.
[8] I. Arsie, M. Graziosi, C. Pianese, G. Rizzo, M. Sorrentino, Proc. 7th Int. Symp. Adv. Vehicle Control (AVEC), Arnhem, The Netherlands, August, 2004.
[9] T. Hofman, R. van Druten, Proc. IEEE Int. Symp. Veh. Power Propulsion, Paris, France, October, 2004.
[10] M. Koot, J. Kessels, B. de Jager, W. Heemels, P. van den Bosch, M. Steinbuch, IEEE Trans. Veh. Technol. 54 (3 (May)) (2005) 771–782.
[11] C. Lin, H. Peng, J.W. Grizzle, J. Kang, IEEE Trans. Control Syst. Technol. 11 (6 (November)) (2003) 839–849.
[12] B. Badreddine, M.L. Kuang, Proc. of Global Powertrain Conference, September, 2004.

[13] V.H. Johnson, K.B. Wipke, D.J. Rausen, in: Proc. Future Car Congress, SAE Paper No. 2000-01-1543, 2000.
[14] R. Langari, J. Won, IEEE Trans. Veh. Technol. 54 (3) (2005) 925–934.
[15] J. Moreno, M.E. Ortúzar, J.W. Dixon, IEEE Trans. Ind. Electron. 53 (2 (April)) (2006) 614–623.
[16] G. Paganelli, G. Ercole, A. Brahma, Y. Guezennec, G. Rizzoni, JSAE Rev. 22 (4 (April)) (2001) 511–518.
[17] A. Sciarretta, L. Guzzella, M. Back, Proc. IFAC Symp. Adv. Automotive Contr., Salerno, Italy, April 19–23, 2004.
[18] F. Syed, M. L. Kuang, J. Czubay, M. Smith, H. Ying, Fuzzy Control to Improve High-Voltage Battery Power and Engine Speed Control in a Hybrid Electric Vehicle, Soft Computing for Real World Applications, NAFIPS, Ann Arbor, MI, June 22–25, 2005.
[19] J.-S. Won, R. Langari, and M. Ehsani, in: Proc. Int. Mech. Eng. Congress and Exposition (IMECE'02), New Orleans, LA, November 2002, pp. IMECE2002-33 460.
[20] J. Won, R. Langari, IEEE Trans. Veh. Technol. 54 (3) (2005) 935–953.
[21] J. Park, Z. Chen, L. Kiliaris, M. A. Masrur, A. Phillips, Y. Murphey, in: 2008 IEEE 68th Vehicular Technology Conference, 22–25 September 2008 Calgary, Canada.
[22] M.M. Freeman, Perspective on hybrid electric technology for future for army vehicles Power Modulator Symposium and 2004 High-Voltage Workshop, Conference Record of the Twenty-Sixth International, May 2004, 2004.
[23] F. Lacressonniere, B. Cassoret, European Conference on Power Electronics and Applications, 11–14 September, 2005.
[24] Matlab Simulink — Simulation and Model-based Design, http://www.mathworks.com/products/simulink/?BB=1.
[25] PSAT (Powertrain System Analysis Toolkit) simulation software, http://www.transportation.anl.gov/software/PSAT/index.html.
[26] P. Atwood, S. Gurski, D.J. Nelson and K. Wipke, Degree of Hybridization Modeling of a Fuel Cell Hybrid Electric Sport Utility Vehicle, SAE paper 2001-01-0236.
[27] M. Kim, H. Peng, J. Power Sources 165 (2007) 819–832.
[28] R. Saeks, C.J. Cox, J. Neidhoefer, P.R. Mays, J.J. Murray, IEEE Trans. Intell. Trans. Syst. 3 (4 (December)) (2002).
[29] Z. Chen, M.A. Masrur, Y. Murphey, Proc. FUZZ-IEEE, June 2008, 2008.
[30] Y. Murphey, T. Chen, B. Hamilton, in: IEEE Trans. Vehicular Technology, vol. 49(1), March 2000, pp. 651–660, Publication Date: March 2000, ISSN:0018-9545.
[31] L.F. Mendonca, J.M.C. Sousa, J.M.G. Sa Da Costa, International Conference of FUZZ-IEEE, 2008.
[32] M. Wang, N. Li, S. Li, International Conference of FUZZ-IEEE, 2008.